Science in China Series B: Chemistry

Springer

www.scichina.com
chem.scichina.com
www.springerlink.com

Synthesis of an AIE-active fluorogen and its application in cell imaging

YU Yong[1,2], HONG YuNing[1], FENG Chao[3], LIU JianZhao[1], LAM Jacky Wing Yip[1], FAISAL Mahtab[1], NG Ka Ming[2], LUO Kathy Qian[2,3†] & TANG Ben Zhong[1,3,4†]

[1] Department of Chemistry, The Hong Kong University of Science & Technology (HKUST), Clear Water Bay, Hong Kong, China;
[2] Department of Chemical and Biomolecular Engineering, HKUST, Clear Water Bay, Kowloon, Hong Kong, China;
[3] Bioengineering Graduate Program, HKUST, Clear Water Bay, Kowloon, Hong Kong, China;
[4] Institute of Biological and Medical Macromolecules, Zhejiang University, Hangzhou 310027, China

A fluorogen named 1-decyl-1-methyl-2,5-bis{4-[(*N*,*N*-diethylamino)methyl]phenyl}-3,4-diphenylsilole (3) was synthesized. It emitted weakly as isolated molecule but strongly as supramolecular aggregate, showing a characteristic behavior of aggregation-induced emission (AIE). The molecules of 3 formed highly emissive nanoparticles in aqueous media, which quickly and selectively marked cytoplasm of HeLa cells and posed no toxicity to the living cells. The fluorogen is thus a promising candidate material for cell imaging as a sensitive, selective and cytocompatible biosensor.

aggregation-induced emission, biosensor, cell imaging

1 Introduction

The development of fluorescence biosensors with high sensitivity, selectivity and biocompatibility is of critical importance to bioscience and biotechnology because it offers a direct visualization tool for detecting biological macromolecules and monitoring biological events under real, living conditions[1−4]. A great variety of materials, such as organic dyes, inorganic quantum dots (QDs) and polymer and silica nanoparticles, have been studied as potential candidates for biosensor applications[1−10].

Organic fluorogens, however, often become weakly fluorescent when they are dispersed in aqueous media or accumulated in living cells, due to the formation of dye aggregates[5,6]. Inorganic QDs are highly emissive and photostable but inherently cytotoxic because they are typically comprised of heavy metals and chalcogens (e.g., CdSe and PbS) [7−9]. The capping agents used in the QD preparations such as trioctylphosphine can also be of biological implication. Similarly, the surfactants used in the fabrications of polymer and silica nanoparticles such as sodium dodecyl sulfate (SDS) are of toxicity concern, because they can stimulate cytolysis processes even at a concentration as low as 0.0005%[10,11].

We have recently discovered a novel phenomenon of aggregation-induced emission (AIE): nonemissive dyes with propeller-shaped molecular structures such as silole, tetraarylethene, fulvene, pyran and polyaryl are induced to emit efficiently by aggregate formation[12−15]. When dispersed in aqueous media, the molecules form highly emissive nanoaggregates, thanks to their AIE attributes. These intriguing properties of the AIE fluorogens have prompted us to explore the possibility of utilizing them as fluorescence biosensors[16,17]. It is envisioned that the AIE nanoparticles can be as emissive as, but much less cytotoxic than, their inorganic QD counterparts.

In this work, we prove that this is indeed the case. We designed and synthesized a new AIE dye named 1-decyl-1-methyl-2,5-bis{4-[(*N*,*N*-diethylamino)methyl]

Received November 30, 2008; accepted December 1, 2008; Published online December 5, 2008
doi: 10.1007/s11426-009-0008-0
†Corresponding author (email: qluo@ust.hk; tangbenz@ust.hk)
Supported by the Research Grants Council of Hong Kong (Grant Nos. 603008, 601608 and 602707), the National Natural Science Foundation of China (Grant No. 20634020) and the CAO GuangBiao Foundation of Zhejiang University.

phenyl}-3,4-diphenylsilole (**3**; Scheme 1). Thanks to the emissive nature of its nanoaggregates in aqueous media, **3** performed as an excellent fluorescence biosensor for cellular imaging, which quickly and selectively stained cytoplasm of living HeLa cells without interfering with their proliferation processes.

2 Experimental

2.1 General information

THF (Labscan) was distilled under dry nitrogen from sodium benzophenone ketyl prior to use. CellTracker™ Green CMFDA (5-chloromethylfluorescein diacetate) was purchased from Molecular Probes. Other chemicals, reagents and solvents were all purchased from Aldrich or Invitrogen and used as received. NMR spectra were taken on a Bruker ARX 400 NMR spectrometer using $CDCl_3$ as solvent. HRMS spectra were recorded on a Finnigan TSQ 7000 triple quadrupole spectrometer operating in a MALDI-TOF mode. Photoluminescence (PL) spectra were recorded on a Perkin-Elmer LS 55 spectrofluorometer. Fluorescence quantum yield (Φ_F) was estimated using 9,10-diphenylanthracene (Φ_F = 0.9 in cyclohexane) as standard. Particle sizes of the silole nanoaggregates in THF/water mixtures were measured on a zeta plus zeta potential analyzer (Brookhaven Instruments).

2.2 Synthesis of functionalized silole derivative 3

The silole derivative **3** was prepared according to the synthetic route shown in Scheme 1. Into a 50 mL round bottom flask were added 0.056 g (8 mmol) of lithium wire and 1.04 g (8 mmol) of naphthalene in 8 mL of dry THF. After stirring at room temperature under nitrogen for 3 h, a deep green solution of lithium naphthalene was formed, which was added dropwise to a solution of 0.77 g (2 mmol) of bis(phenylethynyl)decylmethylsilane (**1**) in 5 mL of THF over 2 min at room temperature. The mixture was stirred for 1 h, cooled to 0℃, and diluted with 10 mL of THF. After addition of 2 g (8 mmol) of $ZnCl_2$·TMEDA, the black suspension was stirred for an additional hour at room temperature. A solution of 2-(4-bromophenyl)ethyldiethylamine (**2**; 1.57 g, 6.6 mmol) and 0.08 g (0.1 mmol) of $PdCl_2(PPh_3)_2$ in 10 mL of THF was then added. After being refluxed overnight and cooled to room temperature, 10 mL of 3 mol/L HCl solution was added and the mixture was extracted with DCM. The combined organic layer was washed with brine and dried over $MgSO_4$. After solvent evaporation under reduced pressure, the crude product was purified by a silica gel column using ethyl acetate/hexane (1:9 *v*/*v*) as eluent. A dark yellow liquid of **3** was obtained in 40% yield. ^{1}H NMR (400 MHz, $CDCl_3$), δ (ppm): 7.11 (m, 4H), 7.00 (m, 6H), 6.91 (m, 4H), 6.84 (m, 4H), 3.50 (m, 4H), 2.54－2.52 (m, 8H), 1.42－1.23 (m, 20H), 1.07－1.04 (m, 13H), 0.50 (s, 3H). ^{13}C NMR (100 MHz, $CDCl_3$), δ (ppm): 154.3, 140.6, 139.1, 138.4, 136.7, 129.9, 128.6, 128.5, 127.2, 125.9, 57.1, 46.6, 32.8, 31.8, 29.5, 29.4, 29.3, 29.1, 23.5, 22.6, 14.0, 13.4, 11.6, –5.2. HRMS (MALDI-TOF), *m*/*e*: 710.5771 ($[M]^+$, calcd 710.4995).

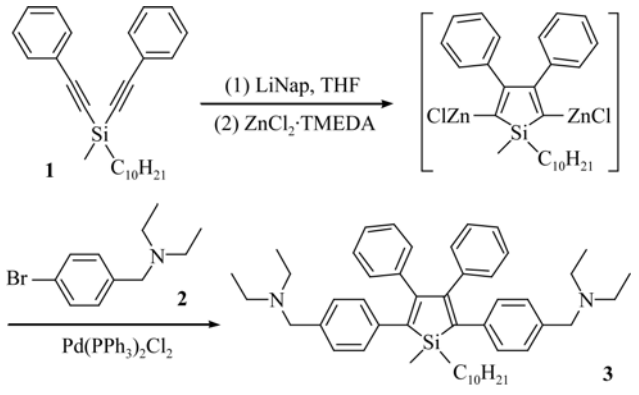

Scheme 1 Synthetic route to functionalized silole derivative **3**.

2.3 Cell culture

HeLa cells were cultured in minimum essential medium containing 10% fetal bovine serum and antibiotics (100 units/mL penicillin and 100 μg/mL streptomycin) in a 5% CO_2 humidity incubator at 37℃.

2.4 Cell imaging

HeLa cells were grown overnight on a plasma-treated 25 mm round cover slip mounted onto a 35 mm Petri dish with an observation window. The living cells were stained with either 5 μmol/L of **3** (by adding 1 μL of a 5 mmol/L stock solution of **3** in DMSO to 1 mL culture) or 5 μmol/L CellTracker™ Green CMFDA for 45 min. The cells were imaged under an inverted fluorescence microscope (Nikon Eclipse TE2000-U) using different combination of excitation and emission filters for each dye: for **3**, Ex = 330－380 nm, diachronic mirror = 400 nm; for Cell Tracker™ Green CMFDA, Ex = 450－490 nm, diachronic mirror = 505 nm. The images of the cells were captured using a computer-controlled SPOT CCD camera (Spot RT SE 18 Mono).

2.5 Cell viability by MTT assay

Viability of the cells was assayed using cell proliferation Kit I with a Perkin-Elmer Victor^3 plate reader at 595 nm. Five thousand cells were seeded per well in a 96-well plate. After overnight culture, various concentrations of **3** were added into the 96-well plate. After 24 h treatment, 10 μL of 3-(4,5-dimethyl-2-thiazolyl)-2,5-diphenyltetrazolium bromide (MTT) solution (5 mg/mL in phosphate buffer solution) was added into each well. After 2 h incubation at 37℃, 100 μL of solubilization solution containing 10% SDS and 0.01 mol/L HCl was added to dissolve the purple crystals. After 24 h incubation, the optical density readings at 595 nm were taken using a plate reader. Each of the experiments was performed at least 3 times.

3 Results and discussion

To check whether **3** is AIE active, we investigated its PL behaviors in pure THF and THF/water mixtures. As can be seen from panel (a) in Figure 1, when a dilute THF solution of **3** is excited at 370 nm, only is a weak PL spectrum recorded by the spectrofluorometer. However, when large amounts of water (>70 vol %) are added to the THF solution, the molecules of **3** start to aggregate and intense PL spectra are obtained under the identical measurement conditions. This confirms that **3** is an AIE fluorogen.

To have a quantitative picture, we measured the Φ_F values of **3** in THF solvent and THF/water mixtures. The Φ_F value remains virtually unchanged when up to ~70 vol % water is added into the THF solution; afterward, it starts to increase swiftly (Figure 1, panel (b)). This proves that the molecularly dissolved species of **3** in pure THF start to form aggregates in the THF/water mixture with a water fraction of ~70% and suggests that the aggregates continue to populate with a further increase in the water fraction in the aqueous mixture. The Φ_F value of the aggregates of **3** in the aqueous mixture with 90% water fraction is ~20%, which is ~10-fold higher than that in the mixture with 70% water.

In our previous work, we found that the absolute Φ_F value of a thin film of 1-methylpentaphenylsilole was 85%[13], which was more than 4-fold higher than the value for its aggregates in the 90% aqueous mixture[12], due to the errors caused by the Mie effect associated with severe light scattering by the silole aggregates. The absolute Φ_F values of the aggregates of **3** thus could be much higher than the relative ones given in Figure 1(b), which were estimated by using 9,10-diphenylanthracene as standard.

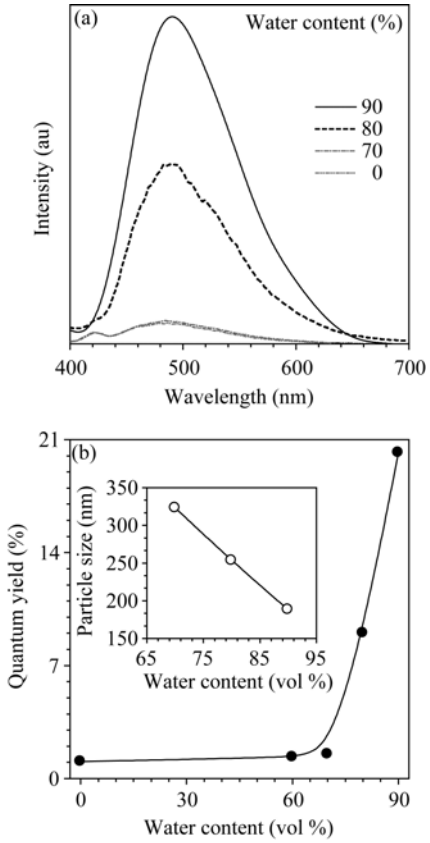

Figure 1 (a) PL spectra of **3** in THF and THF/water mixtures. (b) Dependence of fluorescence quantum yield of **3** on the composition of the THF/water mixture. Inset: effect of solvent composition on the sizes of nanoaggregates of **3** in the aqueous mixture. [**3**] = 10^{-5} mol/L; λ_{ex} = 370 nm.

We investigated the aggregates of **3** by a particle size analyzer. The aggregates are nanosized, as can be seen from the data given in the inset of Figure 1(b), which explains why the aggregate suspensions in the aqueous mixtures are macroscopically homogeneous. Average diameter of the silole nanoaggregates is decreased when the water fraction is increased. In the aqueous mixture with a water fraction of 90%, the average size of the aggregates becomes as small as 188 nm.

Extrapolating from the linear plot given in the inset of Figure 1(b), the molecules of **3** may form even smaller aggregates resembling QDs in size, if the water fraction is further increased to beyond 90%. On the other hand, no accurate and reliable nanoparticle size data can be

obtained in the aqueous mixtures with water fractions lower than 60%: the molecules of **3** may be molecularly dissolved or aggregated into particles too small in size and too few in quantities to be measured by the analyzer.

To function as a useful cell tracer, a fluorogen should neither inhibit nor promote the growth to living cells. As it is known that DMSO exerts no effect on the cell proliferation when its concentration in the medium is below 0.2%, we employed DMSO solutions of **3** with DMSO contents in the media <0.1% in all the biological experiments in this work. As shown in Figure 2, the HeLa cells grow as normally as they do in the control experiment in the presence of **3**. Evidently, **3** is nontoxic to the cells. In other words, it is cytocompatible without interfering with the metabolisms of the living cells.

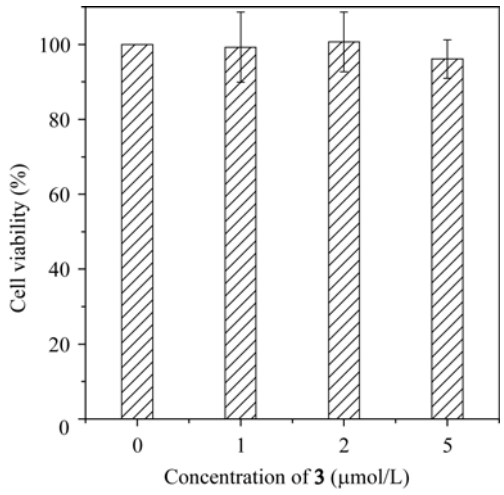

Figure 2 Effect of **3** on the viability of HeLa cells evaluated by MTT assay.

The excellent biocompatibility of **3** encouraged us to utilize it for cell imaging. HeLa cells were imaged by the nanoaggregates of **3** using a standard cell-staining protocol; for comparison, similar experiments were done using a commercial fluorescent dye CellTracker™ Green CMFDA. As shown in Figure 3(a), when the HeLa cells are stained by the aggregates of **3**, the cells are clearly imaged in an exposure time as short as 1 s. Under the identical imaging conditions, CMFDA shows an inferior performance: cell images can hardly be seen when the stained HeLa cells are exposed for 1 s (Figure 3(b)). Clear images can finally be taken when the exposure time is prolonged to 5 s. The image using the nanoaggregates of **3** as cell marker after 5 s exposure, however, is so bright that a proper picture cannot be taken by the microscope.

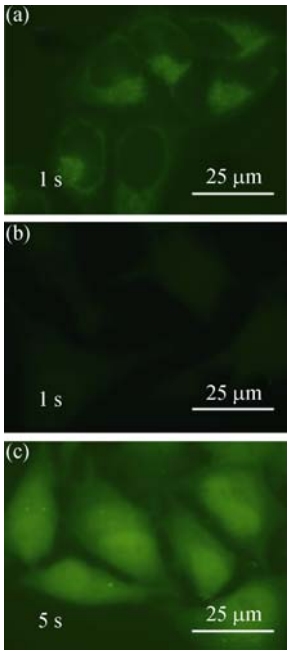

Figure 3 Fluorescence images of HeLa cells stained with (a) **3** and (b, c) CellTracker™ Green CMFDA. Exposure time: (a, b) 1 s; (c) 5 s.

Closer scrutinization of the cell images reveals that the nanoaggregates of **3** stain the cytoplasmic regions of the cells but the CMFDA molecules stain the entire cells. This is probably because the former is hydrophobic but the latter is hydrophilic. Water-soluble fluorogens like CMFDA can pass through the membranes to enter the cells. The small fluorogen molecules can also enter the nucleus via nuclear pores. The water-soluble dyes thus can label both the cytoplasm and nuclear compartments of the cells (Figure 3(c)).

The major route for the nanoaggregates of **3** to enter a living cell is through endocytosis. During this process, the nanoaggregates are enclosed by the cell membrane to form small vesicles that can be internalized by the cell. Inside the cell, the aggregates can be further processed in endosomes and lysosomes and are eventually released from the cellular organelles. The hydrophobic nature of the aggregates prevents them from entering the nucleus of the cell. When the nanoaggregates are bound to the biomacromolecules in the cytoplasm, they become very emissive, due to the additional physical restriction to their intramolecular rotations[18].

The fact that the nanoaggregates of **3** selectively stain the cytoplasmic regions of the cells gives this AIE fluorogen a unique advantage over the CellTracker that stains the entire cells. In most cases of cell imaging, it is necessary to use two different fluorogenic dyes to stain a cell: one to stain DNA in the nucleus of the cell, while

the other to stain the cytoplasmic region surrounding the nucleus. Our newly developed fluorogen **3** is therefore a better choice when used in combination with a DNA-staining fluorogen.

4 Conclusion

In this work, we synthesized a new silole derivative (**3**) with AIE characteristics and demonstrated its utility as a cell-imaging probe. Its nanoaggregates are emissive and cytocompatible. It outperforms a commercial fluorogen of CMFDA and enables sensitive and selective imaging of cytoplasms of living cells. Further investigations on biosensory and cell-imaging behaviors of the aggregates are under way in our laboratories.

1 Wang Y, Shyy J Y J, Chien S. Fluorescence proteins, live-cell imaging, and mechanobiology: Seeing is believing. Ann Rev Biomed Eng, 2008, 10: 1－38

2 Van Engelenburg S B, Palmer A E. Fluorescent biosensors of protein function. Curr Opin Chem. Biol. 2008, 12: 60－65

3 Borisov S M, Wolfbeis O S. Optical biosensors. Chem Rev, 2008, 108: 423－461

4 Domaille D W, Que E L, Chang C J. Synthetic fluorescent sensors for studying the cell biology of metals. Nat Chem Biol, 2008, 4: 168－175

5 Quina F H, Lissi E A. Photoprocesses in microaggregates. Acc Chem Res, 2004, 37: 703－710

6 Capek I. Fate of excited probes in micellar systems. Adv Coll Interf Sci, 2002, 97: 91－149

7 Michalet X, Pinaud F F, Bentolila L A, Tsay J M, S. Doose, Li J J, Sundaresan G, Wu A M, Gambhir S S, Weiss S. Quantum dots for live cells, *in vivo* imaging, and diagnostics. Science, 2005, 307: 538－544

8 Medintz I L, Uyeda H T, Goldman E R, Mattoussi H. Quantum dot bioconjugates for imaging, labelling and sensing. Nat Mater, 2005, 4: 435－446

9 Li H C, Zhou Q F , Liu W, Yan B, Zhao Y B, Jiang G B. Progress in the toxicological researches for quantum dots. Sci China Ser B-Chem, 2008, 51: 393－400

10 Burns A, Ow H, Wiesner U. Fluorescent core-shell silica nanoparticles: Towards "Lab on a Particle" architectures for nanobiotechnology. Chem Soc Rev, 2006,35: 1028－042

11 Krebs F C, Miller S R, Catalone B J, Fichorova R, Anderson D, Malamud D, Howett M K, Wigdahl B. Comparative *in vitro* sensitivities of human immune cell lines, vaginal and cervical epithelial cell lines, and primary cells to candidate microbicides nonoxynol 9, C31G, and sodium dodecyl sulfate. Antimicrob Agents Chemother, 2002, 46: 2292－2298

12 Luo J D, Xie Z L, Lam J W Y, Cheng L, Chen H Y, Qiu C F, Kwok H S, Zhan X W, Liu Y Q, Zhu D B, Tang B Z. Aggregation-induced emission of 1-methyl-1,2,3,4,5-pentaphenylsilole. Chem Commun, 2001, 1740－1741

13 Yu G, Yin S W, Liu Y Q, Chen J S, Xu X J, Sun X B, Ma D G, Zhan X W, Peng Q, Shuai Z G, Tang B Z, Zhu D B, Fang W H, Luo Y. Structures, electronic states, photoluminescence, and carrier transport properties of 1,1-disubstituted 2,3,4,5-tetraphenylsiloles. J Am Chem Soc, 2005, 127(17): 6335－6346

14 Zeng Q, Li Z, Dong Y Q, Di C A, Qin A J, Hong Y N, Ji L, Zhu Z C, Jim C K W, Yu G, Li Q Q, Li Z G, Liu Y Q, Qin J G, Tang B Z. Fluorescence enhancements of benzene-cored luminophors by restricted intramolecular rotations: AIE and AIEE effects. Chem Commun, 2007, 70－72

15 Dong Y Q, Lam J W Y, Qin A J, Li Z, Sun J Z, Sung H H Y, Williams I D, Tang B Z. Switching the light emission of (4-biphenylyl)phenyldibenzofulvene by morphological modulation: Crystallization-induced emission enhancement. Chem Commun, 2007, 40－42

16 Dong Y Q, Lam J W Y, Qin A J, Li Z, Liu J Z, Sun J Z, Dong Y P, Tang B Z. Endowing hexaphenylsilole with chemical sensory and biological probing properties by attaching amino pendants to the silolyl core. Chem Phys Lett, 2007, 446: 124－127

17 Hong Y N, Häuβler M, Lam J W Y, Li Z, Sin K K, Dong Y Q, Tong H, Liu J Z, Qin A J, Renneberg R, Tang B Z. Label-free fluorescent probing of G-quadruplex formation and real-time monitoring of DNA folding by a quaternized tetraphenylethene salt with aggregation-induced emission characteristics. Chem Eur J, 2008, 14: 6428－6437

18 Chen J, Law C C W, Lam J W Y, Dong Y, Lo S M F, Williams I D, Zhu D, Tang B Z. Synthesis, light emission, nanoaggregation, and restricted intramolecular rotation of 1,1-substituted 2,3,4,5-tetra- phenylsiloles. Chem Mater, 2003, 15: 1535－1546